

# Defect-induced effects on carrier migration through one-dimensional poly(*para*-phenylenevinylene) chains

L. Zoppi and A. Calzolari\*

*INFN-CNR-S3, National Center on nanoStructures and bioSystems at Surfaces, I-41100 Modena, Italy*

A. Ruini and A. Ferretti

*INFN-CNR-S3, National Center on nanoStructures and bioSystems at Surfaces, I-41100 Modena, Italy and Dipartimento di Fisica, Università di Modena e Reggio Emilia, I-41100 Modena, Italy*

M. J. Caldas

*Instituto de Física, Universidade de São Paulo, 05508-900 São Paulo, SP, Brazil*

(Received 21 September 2007; revised manuscript received 16 September 2008; published 14 October 2008)

Defects in one-dimensional (1D) systems can be intrinsically distinct from its three-dimensional counterparts, and polymer films are good candidates for showing both extremes that are difficult to individuate in the experimental data. We study theoretically the impact of simple hydrogen and oxygen defects on the electron transport properties of one-dimensional poly(*para*-phenylenevinylene) chains through a multiscale technique, starting from classical structural simulations for crystalline films to extensive *ab initio* calculations within density functional theory for the defects in single crystalline-constrained chains. The most disruptive effect on carrier transport comes from conjugation breaking imposed by the overcoordination of a carbon atom in the vinyl group independently from the chemical nature of the defect. The particular case of the [C=O] (keto-defect) shows in addition unexpected electron-hole separation, suggesting that the experimentally detected photoluminescence bleaching and photoconductivity enhancement could be due to exciton dissociation caused by the 1D characteristics of the defect.

DOI: [10.1103/PhysRevB.78.165204](https://doi.org/10.1103/PhysRevB.78.165204)

PACS number(s): 72.80.Le, 71.20.Rv, 72.40.+w, 73.63.-b

## I. INTRODUCTION

The large variety of interesting properties that can be obtained for crystalline conventional semiconductors is closely related to the possibilities for tuning the transport and optical characteristics through doping and defect control. Conjugated polymers such as poly(*para*-phenylenevinylene) (PPV) present semiconducting characteristics, are optically active in the visible region, and at the same time promise mechanical flexibility, ease, and consequently low cost of fabrication through wet chemistry, motivating thus intensive research worldwide.<sup>1</sup> However, a microscopic understanding of carrier behavior in organic conjugated polymers has been elusive for many years, notwithstanding the large number of experimental and theoretical studies. The discussion covers the intrinsic carrier mobility, holes or electrons,<sup>2-4</sup> exciton migration,<sup>5</sup> and the possibilities for carrier-pair creation and recombination by exciton absorption, emission, or annihilation.<sup>1,5-7</sup> We remark first that the mechanisms for carrier migration are very different from those in conventional semiconductors since the material is not only intrinsically disordered,<sup>8</sup> but also carries strongly anisotropic dimensional characteristics—on-chain and intermolecular—in crystalline grains or amorphous regions.<sup>3,9-11</sup> Also for defects<sup>11</sup> there should be distinct types of environments according to the dimensionality involved. In particular, the influence of on-chain defects due to impurities or conjugation breaking has been much discussed, being often invoked as the reason for the low external efficiency obtained for light-emitting devices. For PPVs, it is known that the detailed morphology is closely tied to the complete formula of the

polymer, including any side-substitution,<sup>12</sup> and that the material is also very sensitive to preparation and operation conditions. One of the main causes of defect incorporation in PPV is indeed photo-oxidation caused by light absorption in air.<sup>13-18</sup> An intriguing observation regarding the formation of carbonyl groups (C=O) in the vinylene segment of PPV is monitored through the vibrational band: there is an undisputed bleaching of photoluminescence (PL),<sup>13</sup> indicating exciton annihilation at defects, and a most unexpected enhancement of photoconductivity (PC).<sup>19</sup> It was soon after suggested<sup>14</sup> that these carbonyl groups (also known as keto-defects) would actually be associated to cleavage of the PPV chain, at the vinylene segment, by creation of two HC=O terminations. As pointed out in Ref. 20 it is not *a priori* granted that these terminations would bleach PL since aldehydes can have high PL yields; however, the cleavage hypothesis has been usually accepted.

Here we focus on oxygen and hydrogen defects in the vinylene segment of single PPV chains. We analyze the defect electronic structure and the impact on the coherent on-chain electron transport. We find that conjugation breaking, the most important cause for the blocking of carrier transport, is mainly induced by the overcoordination of a vinyl carbon atom. *Interestingly, we find that the on-chain keto-defect, with no chain cleavage, presents a surprising electronic structure that can explain both PL bleaching and PC enhancement.*

To discuss the effect of defects on devices, one has to consider independently two issues: (i) the carrier mobility, important for electroluminescence (EL) and PC, and (ii) the formation/recombination of excitons that is predominant in

photoabsorption (PA) and PL phenomena. For both of the above issues the morphology of the organic layer is critical. Chain side-substitution in the active polymeric material is known to affect the morphology and to induce a high degree of disorder in the sample.<sup>12,21</sup> However, for pure unsubstituted PPV it is well known<sup>22</sup> that crystalline grains in herring-bone configuration coexist with amorphous regions. Now, it has been recently shown that the effect of disorder on mobility is not obvious<sup>10</sup> such that carrier mobility can be higher for a more disordered—but more homogeneous—material, while polycrystalline environments are again distinct. This is certainly due to the difference in mobility for along-the-chain vs interchain paths,<sup>3</sup> coupled to the possibility in crystalline domains of charge travel through long segments of linear chains,<sup>9</sup> not expected in disordered regions where interchain hopping mechanisms have performed to dominate: apart from statistical descriptions of carrier mobility, to be applied to the disordered material, the direct atomistic investigation of carrier transport has not been approached yet.

Exciton migration has also been shown to be highly anisotropic<sup>5</sup> and reaches *ca.* 6 nm; excitons are furthermore expected to be attracted to (lower-energy) crystalline regions, and in the specific case of herring-bone PPV sections,<sup>7</sup> we know that the lower-energy exciton is dark and will thus show a longer lifetime and be more prone to be captured at localized exciton traps. While physisorption of oxygen molecules has been associated to the amorphous regions,<sup>17</sup> the on-chain defects are of most interest in the crystalline grains.

We performed an atomistic investigation of defect-state properties and direct on-chain carrier transport for single chains, in the geometrical configuration expected for defects in the bulk crystalline environment. Ours is a multitechnique strategy described in Sec. II. In Sec. III we discuss our results and present our suggestions in the last section.

## II. METHODOLOGY AND COMPUTATIONAL DETAILS

We study the carrier migration processes in defect-containing 1D PPV polymers through two independent points of view. From one hand we discuss the charge trapping mechanisms for electrons and holes induced by the chemical defect, by means of the analysis of the electronic properties of the systems in terms of the localization/delocalization of the single-particle molecular orbitals. On the other hand, we simulate the effect of isolated defects, calculating the quantum transmittance through a simple two-terminal device, constituted of a conduction region (which includes the defect) bridged between two semi-infinite leads (clean polymer chain).

In both cases, the fundamental step is the evaluation of the ground-state electronic properties of the system that we carry out from first principles by means of density functional theory (DFT) calculations, as implemented in the PWSCF code.<sup>23</sup> We adopt gradient-corrected Perdew-Burke-Ernzerhof (PBE) (Ref. 24) exchange-correlation (XC) functional and *ab initio* ultrasoft pseudopotentials.<sup>25</sup> The single-particle electronic wave functions (charge densities) are expanded in a plane-wave basis set, up to an energy cutoff of

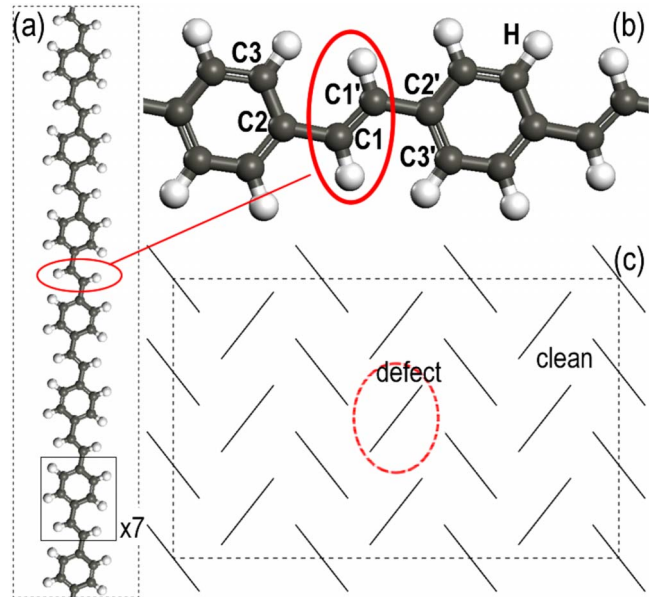


FIG. 1. (Color online) (a) Periodic one-dimensional PPV chain in the unit cell used in DFT calculations, containing seven PPV monomers. The box identifies a single PPV unit. (b) Selected carbon atoms near the vinyl group  $C1=C1'$  [marked by the elliptical box in panel (a)], which hosts the defects. Black and white balls identify C and H atoms, respectively. (c) Monoclinic crystalline arrangement for PPV herring-bone crystals, adopted in force-field calculations. Dashed curved line highlights the unique defect-containing chain.

25 Ry (300 Ry). For Brillouin zone (BZ) integrations we use 30 special  $\mathbf{k}$  points in the irreducible wedge of the 1D BZ of the adopted supercell.

We use supercells with seven-monomer-long PPV segments along the polymer axis [Fig. 1(a)], separated by a thick space of vacuum ( $\sim 15\text{\AA}$ ) in the other two directions. We simulate the defects by chemically modifying the central  $C1-C1'$  vinyl group [labels are defined in Fig. 1(b)] that leaves thus six untouched monomer units between defects.

Geometry optimization of the chains is nontrivial: the atomic relaxation of the defects—in the isolated chain configuration—leads to unphysical overdistorted structures. This is due to the absence of the neighboring polymers that act as steric constraints in the crystal environment. To solve the problem, we prepared a large monoclinic crystalline bulk cell that includes eighteen seven-monomer-long chains in herring-bone configuration,<sup>2,3</sup> into which we then introduce a single defect [Fig. 1(c)].

The huge size of this unit cell ( $\sim 1800$  atoms), along with the poor description with DFT of nonbonded interactions, precludes the use of DFT to optimize the geometry. We adopted a hybrid strategy successfully employed to study other highly packed molecular assemblies.<sup>26,27</sup> We optimize the full in-crystal structure using the classical COMPASS (Ref. 28) force field (FF), which has been explicitly parameterized to predict the structural properties of similar organic molecules in condensed phases. Keeping the atoms fixed in the resulting configuration, we extract from the bulk the defect-containing chain, which we finally study in the iso-

lated phase at the DFT level.<sup>29</sup> The advantages and limitations of this approach are discussed in Ref. 26.

To calculate the coherent transport properties of polymers in the presence of the defects, we follow the Landauer approach that relates the quantum conductance of the conductor (i.e., the inverse of the resistance) to the scattering properties of the system through the expression  $\mathcal{G} = \frac{2e^2}{h} T(E_F)$ , where  $T(E_F)$  is the transmittance at the Fermi energy  $E_F$ . Taking advantage from a real-space description of the problem, the quantum transmittance can be simply expressed as the trace of a matrix product, using the Fisher-Lee expression<sup>30</sup>  $T = \text{Tr}(\Gamma_L G_C^r \Gamma_R G_C^a)$ , where  $G_C^{r,a}$  are the retarded and advanced lattice Green's functions of the conductor region and  $\Gamma_{\{L,R\}}$  represent the coupling between the conductor and the leads. Hence, at least in the zero-bias and zero-temperature regime, the transmittance spectra  $T(E)$  can be evaluated starting from the ground-state electronic structure (i.e., Green's function) of the system.

Here, the transport characteristics are obtained through a real-space implementation of the Landauer formula, in terms of maximally localized Wannier functions (MLWFs),<sup>31,32</sup> using the WANT code.<sup>33,34</sup> After the self-consistent DFT cycle, the resulting plane-wave eigenfunctions are transformed into the real-space Wannier functions. MLWFs are thus used as minimal basis set to calculate the lattice Green's functions that enter into the Fisher-Lee expression<sup>30</sup> used to calculate the quantum transmittance. The details and the applicability of the WANT method are extensively reported elsewhere.<sup>33</sup>

### III. RESULTS AND DISCUSSION

We study the electronic and transport properties of single PPV chains in the presence of two different neutral hydrogen defects. In the first configuration (labeled H-vac) we drop a H atom from a vinyl group, creating a H vacancy in the C1' position [Fig. 2(a)]. In the second case (labeled H-plus) we consider the inclusion of an extra H atom in the C1 position [Fig. 2(b)]. The structural modifications induced by the defects are reported in Table I, along with the corresponding values of the clean (perfect) chain, assumed as reference. In both cases the polymer undergoes a local distortion around the defect that includes the stretching  $\bar{d}_{(11'')}$ , the out-of-plane rotation  $\hat{\theta}_{(3211')}$  of the C1-C1' bond, and the slight torsion of the next-neighbor phenyl rings  $\hat{\theta}_{(322'3')}$ . The effect of the distortion decays almost to zero just one PPV unit away from the defect.

The electronic density of states (DOS) of the clean PPV chain is reported in Fig. 3(a): in agreement with previous theoretical calculations,<sup>3,6</sup> the unperturbed polymer has a semiconducting behavior, and the DOS shows Van Hove singularities, typical of one-dimensional (1D) systems. The single-particle states corresponding to the valence-band top [here denoted as highest occupied molecular orbital (HOMO)] and the bottom of the conduction band [lowest unoccupied molecular orbital (LUMO)] show  $\pi$ -like character, uniformly delocalized over the whole structure, a fingerprint of the charge conjugation in the polymer.

The DOS of H-defect chains are reported in Figs. 3(b) and 3(c). With respect to the clean case, the H-vac and H-plus

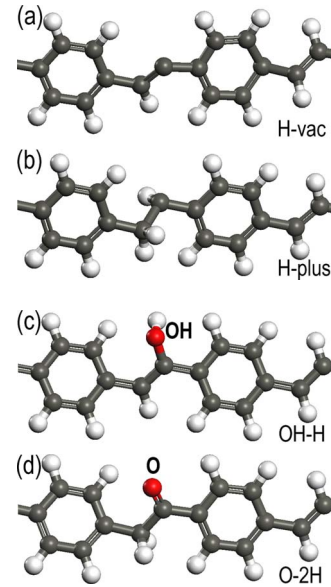


FIG. 2. (Color online) Atomic structure of relaxed PPV chains with defect: zoom on hydrogen [(a)–(b)] and oxygen [(c)–(d)] local defects. The single systems are labeled as in the text.

configurations have one electron less and more, respectively, and a singly-occupied molecular orbital (denoted as SOMO).<sup>35</sup> The H vacancy shifts the Fermi level, partially emptying the top of valence band, and localizes the SOMO around the undercoordinated C1' carbon atom [blue area in Fig. 3(b)]. On the other hand, the inclusion of an extra hydrogen atom in the H-plus configuration overcoordinates the C1 site with respect to the clean configuration, introducing a partially occupied defect state in energy gap of the clean system. Note however, that also in this case the SOMO state remains localized around the C1' atom [blue shaded area in Fig. 3(c)].

These different behaviors reflect on different transport properties as reported in Fig. 4(a), where the zero-bias quantum transmittances are shown. The shaded area represents the transmittance of the clean PPV chain, and we see the plot has a typical steplike behavior. Close to the band edges ( $E \in [-3, 3]$  eV) the transmittance is dominated by a single channel deriving from the  $\pi$  states. Solid and dashed lines correspond to H-vac and H-plus case, respectively. In the H-vac configuration, the presence of an unsaturated bond at the C1' site does not break the charge conjugation along the chain, simply acting as an elastic backscatterer. The corresponding transmittance results to be only partially smoothed with respect to the clean chain, i.e., the H vacancy perturbs only very slightly the electron transport through the chain. On the contrary, the binding of an extra hydrogen atom (H-plus) interrupts the conjugation, blocking the electron flow along the wire: the transmittance is completely depressed in a range of  $\sim 2$  eV below and above the energy gap. Note also that no contributions to quantum transmittance derive from the defect states. In conclusion, despite the presence of partially occupied (localized) states in the gap region, the major wasting effect on transport stems from the overcoordination of the vinyl group that, interrupting the only channel available at these energies, blocks the migration of the charge carriers along the single chain.

TABLE I. Structural parameters for clean and defect-containing chains. Distances  $\bar{d}$  are expressed in Å and torsional angles  $\hat{\theta}$  in degrees; subscript labels refer to carbon atoms as in Fig. 1(b).

	$\bar{d}_{(11')}$	$\bar{d}_{(12)}$	$\bar{d}_{(23)}$	$\bar{d}_{(1'2')}$	$\bar{d}_{(2'3')}$	$\hat{\theta}_{(3211')}$	$\hat{\theta}_{(322'3')}$
Clean	1.36	1.51	1.41	1.51	1.41	4.04	0.51
H-vac	1.52	1.50	1.41	1.53	1.37	23.05	2.16
H-plus	1.54	1.52	1.40	1.51	1.41	-47.30	2.92
OH-H	1.37	1.51	1.41	1.51	1.41	28.46	4.91
O-2H	1.51	1.53	1.40	1.51	1.40	33.79	19.88

We now turn to oxygen defects for which we studied two systems: in the first case (labeled OH-H) we consider the insertion of an oxygen atom, forming a hydroxyl (OH-) termination to the C1' site, as shown in Fig. 2(c). In the second geometry (labeled O-2H) we considered migration of the H atom from the OH-group to the C1 carbon atom, leading to a carbonyl C1'=O and a C1-H<sub>2</sub> termination at the C1-C1' bond [Fig. 2(d)]. The latter geometry corresponds to the keto configuration and results energetically stable with respect to the former enol form (OH-H), as found for most ketones.

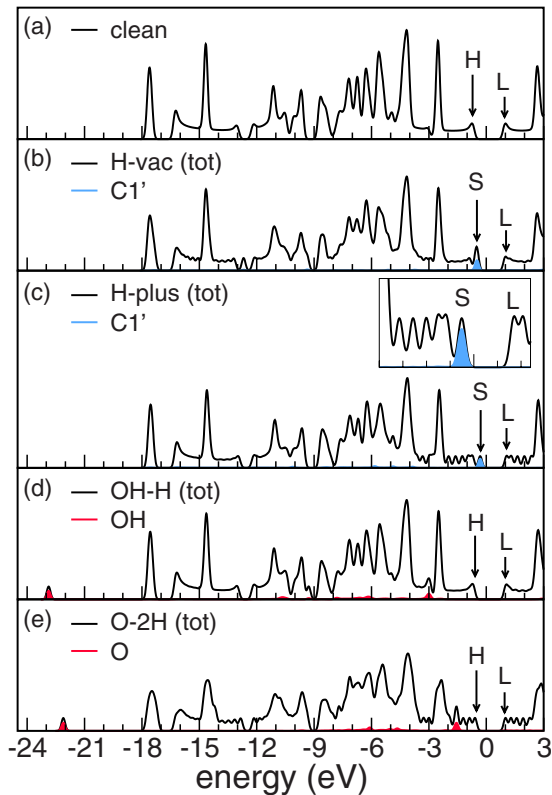


FIG. 3. (Color online) Total (black line) and projected (shaded area) density of states of the clean chain (a), chain with hydrogen defect (b-c), and oxygen defect (d-e) defected systems. Light blue areas in panels (b)–(c) correspond to the DOS projected on atom C1' [label follows Fig. 1(b)]. Red areas in panels (d)–(e) mark the projection on the oxygen atom. Arrows identify HOMO (h), SOMO (s), and LUMO (l) peaks. Plots for the defectcontaining systems are aligned to DOS of the clean chain, assumed as the reference. The zero of the energy corresponds to the calculated Fermi energy of the clean system. Inset of panel (c) zooms on the defect state in the gap.

The OH-H configuration is however important since it is expected to be the first step of the oxygen insertion reaction; the barrier describing the probability of interconversion between the two tautomers was calculated from first principles for the prototype case of acetone.<sup>36</sup>

The two configurations with oxygen-defect are isoelectronic, with an even number of electrons, and in both cases the HOMO and the LUMO carry  $\pi$  character, and no further states are introduced in the gap.<sup>37</sup> The oxygen-derived states [red shaded area in Figs. 3(d) and 3(e)] are  $\sim 2$  eV below the top of the valence band for both defects. On the contrary, the transport properties are very different in the two systems: we can see from the quite smooth DOS in Fig. 3(d) that, despite the drastic structural modifications, the hydroxy-defect changes only very slightly the electronic properties of the system, while the DOS for the keto-defect near the band edges shows a rugged appearance, similar to the H-plus case. In fact, for the OH-H phase, the transmittance [straight line in Fig. 4(b)] is essentially the same as for the clean chain, while it is dramatically reduced in the keto-defect. The hydroxyl defects have no effects on the charge transport, while the keto-defect completely blocks the ballistic charge flow along the polymer. As we did for the hydrogen defect, we can relate these characteristics to the coordination state of the defect containing vinyl group: the OH-H configuration, despite the presence of the oxygen atom, maintains the formal coordination of both C1 and C1' sites of the central vinyl and does not present modifications in the transport proper-

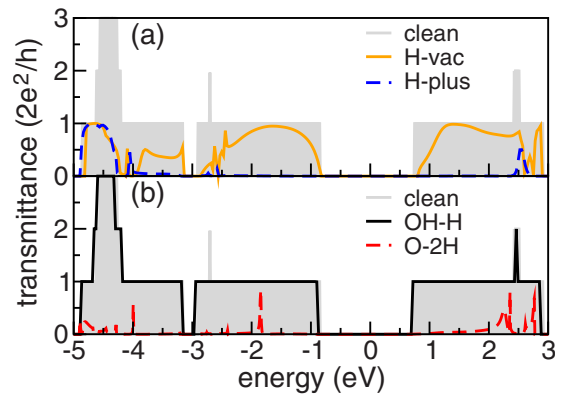


FIG. 4. (Color online) (a) Quantum transmittance for H-vac (solid) and H-plus (dashed) systems. (b) Quantum transmittance for PPV chains with oxygen defect: OH-H (solid) and O-2H (dashed). Shaded squarelike area in both panels corresponds to the transmittance of the clean system.

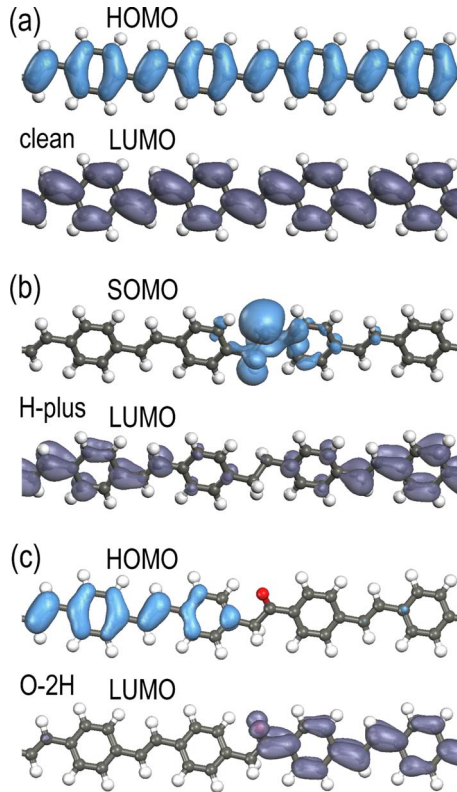


FIG. 5. (Color online) Isosurface plots of selected frontier orbitals for clean (a), H-plus (b), and O-2H (c) systems. Light and dark blue plots correspond to occupied and empty states, respectively.

ties, as indeed found experimentally.<sup>20</sup> The O-2H system, instead, overcoordinates both sites, breaking charge conjugation and the conductivity of the single chain, as in the H-plus case. In summary, while the electronic properties of the defect system depends on the chemical nature of the impurity, the mechanism that rules the on-chain transport depends mainly on the overcoordination of a vinyl carbon atom that breaks the  $\pi$ -charge conjugation, independently from the type of defect that caused it.

The analysis above demonstrates that both the H-plus and the O-2H defect inhibit the coherent electron transport along the chain in a similar way, while interchain hopping processes can still occur and in this sense these defects can be thought similar to a chain break. However, a deeper analysis of the electronic structure indicates possible different mechanisms for PL bleaching and PC responses. The presence of defects can cause severe distortion in the geometry of the chain, in particular in the torsional angles between neighbor phenylene units (see Table I). The specific distortion is characteristic of each defect, and in particular it is different for the two overcoordinated defects, H-plus and O-2H: for the H-defect the result is a large angle between the bridging carbon atoms and the neighbor phenylene rings ( $3211^\circ$ , Table I), which will help to localize the defect state, while in the case of the keto-defect the torsion evolves from one phenylene unit across the bridge to the other unit. In Fig. 5 we compare the frontier orbitals of the clean, H-plus and O-2H configurations. We see that the H-plus center introduces a very localized defect state, extending just over one monomer

unit, as found for other conjugated systems.<sup>38</sup> The keto-defect on the other hand introduces a barrier in the 1D chain, with the hole-related state arriving up to the phenylene unit before the defect, and the electron-related state starting just across at the lone pair of the oxygen atom and proceeding forward; both states are perfectly conjugated up to the defect and do not overlap at all (Fig. 5). We recall that the first singlet exciton in clean PPV is direct (electron and hole on one chain, even in the herring-bone crystal) with a binding energy of  $\sim 0.5$  eV; mostly composed of the edge  $\pi$  states, it extends over *ca* six monomers.<sup>7</sup> Furthermore, as said before, the 3D herring-bone chain arrangement found for the case of pristine PPV is associated with an absence of optical activity for the lowest direct exciton that is found to be dark by symmetry:<sup>7</sup> as such, the electron-hole pair can travel far and be easily captured by traps before recombining or relaxing. We infer that the presence of a H-plus defect could trap and destroy an exciton by nonradiative decay (phonon emission) at the defect center: photo-created pairs are annihilated. As for the keto-defect, the incoming exciton is expected to easily *split in an electron and a hole, free to proceed in separate ways along the chain*, which would strongly improve the photoconductivity efficiency of the sample.

#### IV. CONCLUSIONS

Concluding, we studied important chemical defects on un-cleaved PPV single chains in the configurations expected for herring-bone crystalline regions. For the H-related defects, we find that the missing H atom does not affect very much either the electronic structure or the carrier transport characteristics, while the over-coordination through insertion of an additional H atom presents the expected strong effects with inclusion of a localized defect state and transport blocking due to conjugation break. This indicates that exposure to air and water vapor can be damaging to device operation (be it for light emission or absorption) due to the presence of the  $H^+$  proton typical of moisture conditions. On the contrary, the simple insertion of an oxygen atom in the CH termination (leading to a hydroxyl group) does not introduce localized traps or affect carrier transport.

While for the H defects and the hydroxyl case we find typical defect structures, we obtain a completely different picture for the keto-defect, which is specific to the one-dimensional symmetry of the system, and can lead to exciton splitting in free carriers. This very unexpected picture can explain why the hydroxyl centers apparently do not cause any disturbance to electronic and optical properties, while keto-defects at once bleach the photoluminescence and enhance photoconductivity.

In summary, these findings lead to a reframing of the role of defects in organic materials, suggesting that in this particular case, for PPV, where herring-bone crystallites should be avoided for light-emitting devices, the proper oxidation of the same crystallites could be useful for photovoltaic applications.

#### ACKNOWLEDGMENTS

We would like to thank E. Molinari and C. Cavazzoni for

fruitful discussions and technical support. This work was funded in part by the Regional Laboratory of Emilia Romagna “Nanofaber,” and by the Italian MIUR through Contract No. PRIN 2006. M.J.C. acknowledges support from FAPESP

and CNPq, Brazil, and INFM-CNR, Italy. Access to the CI-NECA supercomputing facilities was granted by INFM-CNR.

\*Corresponding author: calzolari.arrigo@unimore.it

- <sup>1</sup>R. Friend, R. Gymer, A. Holmes, J. Burroughes, R. Marks, C. Taliani, D. Bradley, D. D. Santos, J. Brédas, M. Lögdlung, and W. Salaneck, *Nature (London)* **397**, 121 (1999).
- <sup>2</sup>A. Ferretti, A. Ruini, E. Molinari, and M. J. Caldas, *Phys. Rev. Lett.* **90**, 086401 (2003).
- <sup>3</sup>A. Ferretti, A. Ruini, G. Bussi, E. Molinari, and M. J. Caldas, *Phys. Rev. B* **69**, 205205 (2004).
- <sup>4</sup>J. Cornil, J.-L. Brédas, J. Zaumseil, and H. Sirringhaus, *Adv. Mater. (Weinheim, Ger.)* **19**, 1791 (2007).
- <sup>5</sup>D. E. Markov and P. W. M. Blom, *Phys. Rev. B* **74**, 085206 (2006).
- <sup>6</sup>M. Rohlfiing and S. G. Louie, *Phys. Rev. Lett.* **82**, 1959 (1999).
- <sup>7</sup>A. Ruini, M. J. Caldas, G. Bussi, and E. Molinari, *Phys. Rev. Lett.* **88**, 206403 (2002).
- <sup>8</sup>I. H. Campbell, B. K. Crone, and D. L. Smith, *Semiconducting Polymers: Chemistry, Physics and Engineering*, Physics of Organic Light-Emitting Diodes Vol. 2, 2nd ed. (Wiley, Weinheim, 2007), pp. 421–454.
- <sup>9</sup>R. A. Street, J. E. Northrup, and A. Salleo, *Phys. Rev. B* **71**, 165202 (2005).
- <sup>10</sup>Y.-F. Huang, A. Inigo, C.-C. Chang, K.-C. Li, C.-F. Liang, C.-W. Chang, T.-S. Lim, S.-H. Chen, J. White, U.-S. Jeng, A.-C. Su, Y.-S. Huang, K.-Y. Peng, S.-A. Chen, W.-W. Pai, C.-H. Lin, A. Tameev, S. Novikov, A. Vannikov, and W.-S. Fann, *Adv. Funct. Mater.* **17**, 2902 (2007).
- <sup>11</sup>J.-F. Chang, H. Sirringhaus, M. Giles, M. Heeney, and I. McCulloch, *Phys. Rev. B* **76**, 205204 (2007).
- <sup>12</sup>M. Kemerink, J. van Duren, P. Jonkheijm, W. Pasveer, P. Koenderaad, R. Janssen, H. Salemink, and J. Wolter, *Nano Lett.* **3**, 1191 (2003).
- <sup>13</sup>F. Papadimitrakopoulos, K. Konstadinidis, T. M. Miller, R. Opila, E. A. Chandross, and M. E. Galvin, *Chem. Mater.* **6**, 1563 (1994).
- <sup>14</sup>R. D. Scurlock, B. Wang, P. R. Ogilby, J. R. Sheats, and R. L. Clough, *J. Am. Chem. Soc.* **117**, 10194 (1995).
- <sup>15</sup>N. T. Harrison, G. R. Hayes, R. T. Phillips, and R. H. Friend, *Phys. Rev. Lett.* **77**, 1881 (1996).
- <sup>16</sup>F. Janssen, L. van IJzendoorn, H. Schoo, J. Sturm, G. Andersson, A. D. van der Gon, H. Brongersma, and M. de Voigt, *Synth. Met.* **131**, 167 (2002).
- <sup>17</sup>H.-E. Tseng, K.-Y. Peng, and S.-A. Chen, *Appl. Phys. Lett.* **82**, 4086 (2003).
- <sup>18</sup>S. Chambon, A. Rivaton, J.-L. Gardette, M. Firon, and L. Lutsen, *J. Polym. Sci., Part A: Polym. Chem.* **45**, 317 (2007).
- <sup>19</sup>H. Antoniadis, L. J. Rothberg, F. Papadimitrakopoulos, M. Yan, M. E. Galvin, and M. A. Abkowitz, *Phys. Rev. B* **50**, 14911 (1994).
- <sup>20</sup>L. Rothberg, M. Yan, F. Papadimitrakopoulos, M. Galvin, E. Kwock, and T. Miller, *Synth. Met.* **80**, 41 (1996).
- <sup>21</sup>M. Kemerink, J. van Duren, A. van Breemen, J. Wildeman, M. Wienk, P. W. M. Blom, H. Schoo, and R. Janssen, *Macromolecules* **38**, 7784 (2005).
- <sup>22</sup>P.-K. Wei, Y.-F. Lin, W. Fann, Y.-Z. Lee, and S.-A. Chen, *Phys. Rev. B* **63**, 045417 (2001).
- <sup>23</sup>S. Baroni, A. Dal Corso, S. de Gironcoli, and P. Giannozzi, 2001, <http://www.pwscf.org>.
- <sup>24</sup>J. P. Perdew, K. Burke, and M. Ernzerhof, *Phys. Rev. Lett.* **77**, 3865 (1996).
- <sup>25</sup>D. Vanderbilt, *Phys. Rev. B* **41**, 7892 (1990).
- <sup>26</sup>A. Calzolari, A. Ruini, E. Molinari, and M. J. Caldas, *Phys. Rev. B* **73**, 125420 (2006).
- <sup>27</sup>M. Caldas, A. Calzolari, and C. Cucinotta, *J. Appl. Phys.* **101**, 081719 (2007).
- <sup>28</sup>H. Sun, *J. Phys. Chem. B* **102**, 7338 (1998).
- <sup>29</sup>We decided for optimizing just with classical importance of van der Waals interactions of this approach for such systems states. See also 2006.
- <sup>30</sup>D. S. Fisher and P. A. Lee, *Phys. Rev. B* **23**, 6851 (1981).
- <sup>31</sup>N. Marzari and D. Vanderbilt, *Phys. Rev. B* **56**, 12847 (1997).
- <sup>32</sup>A. Ferretti, A. Calzolari, B. Bonferroni, and R. Di Felice, *J. Phys.: Condens. Matter* **19**, 036215 (2007).
- <sup>33</sup>A. Calzolari, N. Marzari, I. Souza, and M. Buongiorno Nardelli, *Phys. Rev. B* **69**, 035108 (2004).
- <sup>34</sup>A. Calzolari, A. Ferretti, C. Cavazzoni, N. Marzari, and M. Buongiorno Nardelli, 2005, WANT code, <http://www.wannier-transport.org>.
- <sup>35</sup>The explicit treatment of the spin degrees of freedom does not change the characteristics of the systems, at least within the local spin density approximation.
- <sup>36</sup>C. Cucinotta, A. Ruini, A. Catellani, and A. Stirling, *ChemPhysChem* **7**, 1229 (2006).
- <sup>37</sup>The inclusion of self-energy corrections beyond the standard DFT approach, e. g., within GW, could modify the energy position of the localized defect levels with respect to the gap. However, an accurate energy calculation for such isolated defect states would not affect the transport properties of the system, going beyond the aim of this work.
- <sup>38</sup>J. E. Northrup and M. L. Chabiny, *Phys. Rev. B* **68**, 041202(R) (2003).